Structural and electronic properties of *h*-BN

Lei Liu, Y. P. Feng, and Z. X. Shen

Physics Department, National University of Singapore, 2 Science Drive 3, 117542 Singapore
(Received 20 February 2003; published 2 September 2003)

Effects of stacking behavior of hexagonal basal layers to the structural stability and electronic properties of *h*-BN were investigated thoroughly using first-principles calculations based on the density-functional theory local-density approximation. Three of five possible *h*-BN structures with ''good'' stacking were found to be stable or substable. Considering that intrinsic stacking fault exist in real *h*-BN crystals which results in mixed stacking behavior, the experimentally observed large interlayer spacing of structures with stacking disorder such as PBN and *t*-BN can be understood. A substable structure with a direct band gap of about 3.395 eV was predicted. The existence of this substable structure and related intrinsic stacking fault in real *h*-BN explains the discrepancy in the nature of the band gap and the large variation in the observed band-gap values of *h*-BN.

I. INTRODUCTION

Being one of the most interesting solids among the III-V compounds, boron nitride (BN) has motivated tremendous amounts of theoretical and experimental investigations of its fundamental properties for a long time.[1–15] BN is also the basis for many advanced technologies.[16] Four different polymorphic modifications, i.e., cubic (*c*-BN), wurzite (*w*-BN), hexagonal (*h*-BN), and rhombohedral (*r*-BN), have been found for BN which are responsible for the wide spectrum of properties of BN.[16] The two high-density diamondlike phases, *c*-BN and *w*-BN, have tetrahedral sp^3 hybridized B-N bonds, but different stacking sequences of the BN basal layers. The *c*-BN consists of the three-layer (ABCABC$\cdots$) stacking of the *c*-BN (111) planes while *w*-BN follows the two-layer (AA′AA′$\cdots$) stacking sequence of *w*-BN (0002) planes which is structurally identical to the *c*-BN (111) planes.[16–18] The two low-density graphitelike phases, *h*-BN and *r*-BN, consist of two-dimensional layers of hexagonally linked sp^2 hybridized B-N bonds, arranged in (aa′aa′$\cdots$) and (abcabc$\cdots$) orders, respectively.[16–18] In addition to the above, BN has been found to exist in partial or completely disordered phases. The turbostratic (*t*-BN) (Refs. 18–21) phase has random stacking of the hexagonal sp^2 bonded BN basal layers and is a partially disordered phase, while amorphous BN (*a*-BN) is characterized by atomic-level structural disorders.[18] The most common phase of boron nitride, *h*-BN, is known as a very good electrical insulator with good thermal conductivity and stability. It has been widely used in vacuum technology and also been employed in electronics, nuclear energy, x-ray lithography, lubrication, etc.[22,23]

Despite the fact that *h*-BN is the best studied polymorph of BN, there has been no agreement on the basic electronic properties of *h*-BN to date. For example, there is a wide range of values for its band-gap energy.[22] Electronic states of *h*-BN have been studied by luminescence,[1,2,6,9,22,24] electron energy-loss spectroscopy,[25–27] x-ray photoemission spectroscopy,[28,29] x-ray emission,[30,31] x-ray absorption,[12,32] resonant inelastic x-ray scattering,[33,34] optical-absorp-

tion[13,35–37] and reflectivity spectra,[4,38,39] and other techniques.[40,41] However, widely dispersed band-gap energy values ranging from 3.6 eV to 7.1 eV can be found in the literature and both direct or indirect band gaps have been reported for *h*-BN.

Meanwhile, extensive theoretical studies have been performed on the electronic and optical properties of *h*-BN. However, the calculated band structures are dependent on the calculation methods. Using the tight-binding method, Robertson investigated the electronic structure and core excitation of *h*-BN and found a direct gap at the *H* point, but a very small *K-H* dispersion.[42] Calculation based on the full-potential self-consistent linearized augmented-plane-wave method by Catellani *et al.* showed that *h*-BN has a minimal indirect band gap of 3.9 eV between the valence-band maximum at *H* and the conduction-band minimum at *M*, and a lowest direct band gap of 3.9 eV at *H*.[43] However, Park *et al.* found that the lowest direct gap of *h*-BN is located at *M*, with a gap value of 4.5 eV using the same method.[44] Results of band-structure calculations based on the orthogonal linear combination of atomic orbitals (OLCAO) method by Xu and Ching suggest an indirect band gap (*H-M*) of 4.07 eV and a lowest direct band gap (*H*) of 4.2 eV.[45] Using a pseudopotential approach, Furthmüller *et al.* predicted a direct gap of 4.5 eV at the *M* point, which is 0.4-eV larger than the indirect gap between the *M* and *H* points.[46]

While these studies provided a certain degree of understanding of the electronic properties of *h*-BN, few of them directly addressed the conflicting experimental and theoretical values of the fundamental band gap of *h*-BN. Sample quality was often cited as the reason for the great variation in the electronic properties from sample to sample. Although many investigations on the electronic properties of *h*-BN, such as defects,[8,10,47,48] core hole effect,[33,34,49] and luminescence,[1,2,6,9,22,24] were carried out, it is difficult to give an accurate description without fully understanding the band structure of *h*-BN.

It was unfortunate that nearly all experimental analyses or theoretical calculations on *h*-BN were based on the hexagonal crystal structure first proposed by Pease,[50,51] as shown in
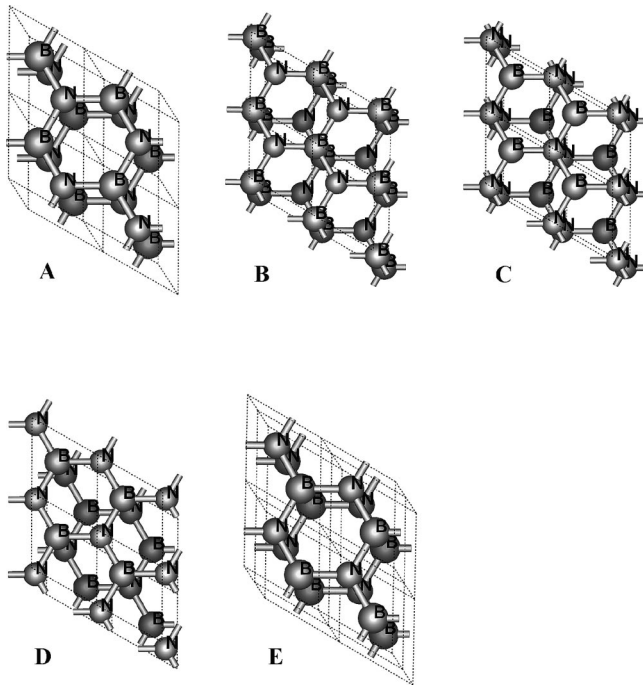
FIG. 1. *h*-BN structures considered in this study. Structures A, B, and C all have space group $P6_3/mmc$ (194) and can be transformed into one another by translational gliding moves of the BN plane. Structure D with the space group $P3m1$ (156) and structure E with the space group $P\bar{6}m2$ (187) are similarly related.

TABLE I. *h*-BN crystal structures determined by XRD.

Space group	a (Å)	c (Å)	Reference
$P6_3/mmc$ (194)	2.50441(7)	6.6522(4)	52
$P\bar{6}m2$ (187)	2.502(2)	6.66(1)	53
$P\bar{6}m2$ (187)	2.50399(5)	6.6612(5)	54
$P\bar{3}m1$ (164)	2.502(2)	6.66(1)	55
$P\bar{3}m1$ (164)	2.5000(1)	6.6609(5)	56
$P\bar{3}m1$ (164)	2.51	6.69	57
$P\bar{6}$ (174)	2.51	6.69	58

tion of structural and electronic properties of *h*-BN related to stacking of the basal BN layers using the density-functional theory[60,61] (DFT) and the local-density approximation[61] (LDA), and aim to provide a clear understanding of the structural and electronic properties of *h*-BN, as well those of PBN and *t*-BN.

II. STRUCTURAL PROPERTIES OF *h*-BN WITH DIFFERENT STACKING

According to the XRD data, a few different types of *h*-BN ($Z=2$) with space groups of $P6_3/mmc$ (194),[52] $P\bar{6}m2$ (187),[53,54] $P\bar{3}m1$ (164),[55–57] and $P\bar{6}$ (174)[58] as shown in Table I, are possible. However, based on symmetry consideration, there can be only five hexagonal *h*-BN structures ($Z=1$ or 2). These five structures are shown in Fig. 1 and the corresponding space groups are $P6_3/mmc$ (194) for structures A, B, and C; $P3m1$ (156) for structure D; and $P\bar{6}m2$ (187) for structure E. We suggest that the *h*-BN structures with the $P\bar{3}m1$ (164) (Refs. 55–57) symmetry observed experimentally should be denoted $P3m1$ (156), because it is impossible for *h*-BN ($Z=2$) to have the $P\bar{3}m1$ (164).

Among the five possible structures, structure A with the $P6_3/mmc$ is most commonly accepted. These five structures can be transformed into each other, by translational gliding moves of one BN basal layer relative to the other layer in the unit cell, or by rotational moves of one BN basal layer around the *c* axis of the crystal. However, if only translational moves are permitted, then the five *h*-BN structures can be divided into two groups. The first group (I) consists of structures A, B, and C with the space group $P6_3/mmc$, and the second group (II) is composed of structures D and E with the space groups $P3m1$ and $P\bar{6}m2$, respectively. In each group, the *h*-BN structures can transform into each another by varying the relative stacking of the BN basal layers.

Theoretical investigations on the structural and electronic properties of *h*-BN were carried out using a first-principles method based on the DFT, and the LDA with the Perdew-Zunger parametrization[62] for the exchange and correlation interaction. Each *h*-BN structure was optimized within the given space group using the CASTEP code.[63] The ultrasoft pseudopotential[64] was used in our calculation and the electron wave function was expanded using plane waves with a

Fig. 1(A). In this crystal structure which has space group $P6_3/mmc$ (194), the hexagonal BN layers align in the *c* direction in such a way that the hexagons reside directly above one another and the B atoms immediately above the N atoms or vice versa. However, for real *h*-BN crystals ($Z=2$), x-ray-diffraction (XRD) data indicate that the crystal may exist in structures with different symmetries. In particular, *h*-BN structures with space groups $P6_3/mmc$ (194),[52] $P\bar{6}m2$ (187),[53,54] $P\bar{3}m1$ (164),[55–57] and $P\bar{6}$ (174),[58] respectively, have been found. In fact, Geick *et al.* discussed their optical investigation data in terms of two *h*-BN structures with different stacking sequences of the hexagonal BN layers in 1960s.[4] However, few theorists have paid attention to the stacking effects of the structural and electronic properties of *h*-BN since then, except a recent work by Mosuang and Lowther which indicated that slightly different phases of this material could exist in three forms of the AaAa··· stacking.[59] Moreover, stacking disorder was found in pyrolytic boron nitride (PBN) formed by chemical vapor deposition and in the semicrystalline BN phase, *t*-BN, where larger interlayer spacing was observed.[16,20] However, to our best knowledge there has been no theoretical study on the structural or electronic properties of PBN and *t*-BN. Therefore, it would be interesting to investigate the structural stability of *h*-BN related to the stacking behavior of hexagonal basal layers. It could elucidate the uncertainty of the band structure of *h*-BN observed experimentally, and provide further understanding of the electronic properties of PBN and *t*-BN.

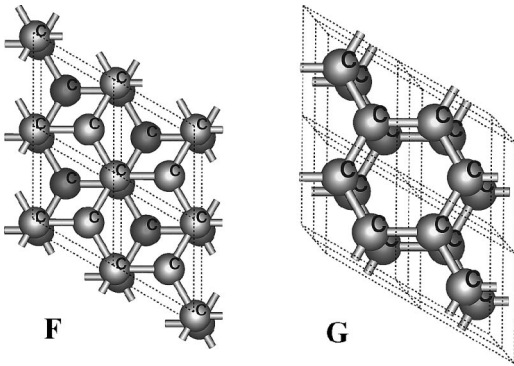In this paper, we report results of a systematic investiga-

FIG. 2. Graphitic structures for reference. The two structures F and G have the space groups $P6_3/mmc$ (194) and $P6/mmm$ (191), respectively.

kinetic-energy cutoff of 540 eV. K points were generated using the Monkhorst-Pack scheme with a mesh size of 12 $\times 12 \times 4$. With these parameters, the accuracy in the calculated total energy is estimated to be 0.001 eV per atom. In addition to the five h-BN structures, two graphitic structures with hexagonal symmetry were also studied for comparison. These two structures, F with space group $P6_3/mmc$ (194) and G with space group $P6/mmm$ (191), are shown in Fig. 2. The calculated total energies per atom and the lattice parameters of these structures are listed in Table II. The optimized structures A, B, and D have similar lattice parameters a and c, which are in good agreement with the experimental results given in Table I. Their total energies per atom are also close. On the other hand, the optimized structures C and E have a relatively larger lattice constant c, and relatively higher total energies per atom. Similarly, in the case of graphite, structure F, the common graphitic structure, has lower total energy and a much shorter lattice constant c than structure G.

Compared with hexagonal graphite which has only one stable structure, i.e., structure F, h-BN has three possible stable structures, i.e., structures A and B, both of the $P6_3/mmc$ (194) symmetry, and D with $P3m1$. This could be due to the characteristics of the mixed covalent-ionic bonding of h-BN, in contrast to pure covalent bonding of graphite. As shown in Fig. 3, where the total valence charge density of the five h-BN structures and the two graphitic structures are shown using contour plots in the (1100) plane containing both BN and CC bonds, all h-BN and graphitic

structures have strong bonding in the ab plane but weak bonding in the c direction. This is a result of strong covalent intralayer bonds and weak interlayer Van der Waals bonding. In the case of graphitic structures which show pure covalent bonding characteristics, the charge density is distributed equally around the C atoms [Fig. 3 (structures F and G)] and the interlayer van der Waals interaction favors a stacking sequence in which the hexagonal graphitic rings in adjacent layers are shifted, i.e., the ABAB stacking sequence. However, in the case of h-BN which shows mixed covalent-ionic bonding characteristics, the valence charges are concentrated around the N atoms [Fig. 3(structures A–E)] and the layer stacking in the three h-BN structures A, B, and D yield local energy minima.

To further investigate the stability of these five h-BN structures, we calculated the variation of the total energy per atom of the structures in each group as a function of the relative translational move of one basal BN layer with respect to the other in the unit cell. For the group-I structures, as shown in Fig. 4, structure A was found to be a stable structure and its energy per atom is at the global minimum. Structure B is a substable phase and its energy is at a local minimum which is only slightly higher than that of structure A. But structure C is unstable since its energy is at the maximum point of the energy surface. The equilibrium structure of C has a relatively longer lattice parameter c, as shown in Table II. The group-II structures, D and E, show similar behaviors. As shown in Fig. 5, structure D is a stable structure at the minimum point of total energy, but structure E is unstable at the maximum point of total energy. The equilibrium structure of E also has a longer lattice constant c, as indicated in Table II. Recently, Mosuang and Lowther investigated, using a density-functional approach with LDA, three BN phases with different stacking sequences which correspond to structures A, C, and E here. However, they concluded that all three structures were stable. This could be due to the fact that an interlayer gliding effect was not considered in their study.

According to our results presented above, among the five structures of h-BN, structures A, B, and D are stable and the corresponding stacking of the BN layers can be regarded as energetically favorable or "good" stacking sequences. Structures C and D are unstable and their stacking sequences can be regarded as unfavorable or "bad." Structures with "bad" stacking sequence generally have larger c values compared to structures with "good" stacking sequences. The five struc-

TABLE II. Calculated structural information and total energies of various h-BN structures.

| Group	Structure	Space Group	a (Å)	c (Å)	Total energy (eV/atom)	Stability	E_g (eV)
h-BN	A	$P6_3/mmc$ (194)	2.485	6.49	−175.849	stable	4.027 (indirect)
Group I	B	$P6_3/mmc$ (194)	2.484	6.487	−175.847	substable	3.395 (direct)
	C	$P6_3/mmc$ (194)	2.484	7.048	−175.837	unstable	3.433 (indirect)
h-BN	D	$P3m1$ (156)	2.485	6.423	−175.849	stable	4.208 (indirect)
Group II	E	$P\bar{6}m2$ (187)	2.485	6.912 (×2)	−175.835	unstable	3.226 (indirect)
Graphite	F	$P6_3/mmc$ (194)	2.439	6.654	−155.560	stable	
	G	$P6/mmm$ (191)	2.439	7.234 (×2)	−155.548	unstable	
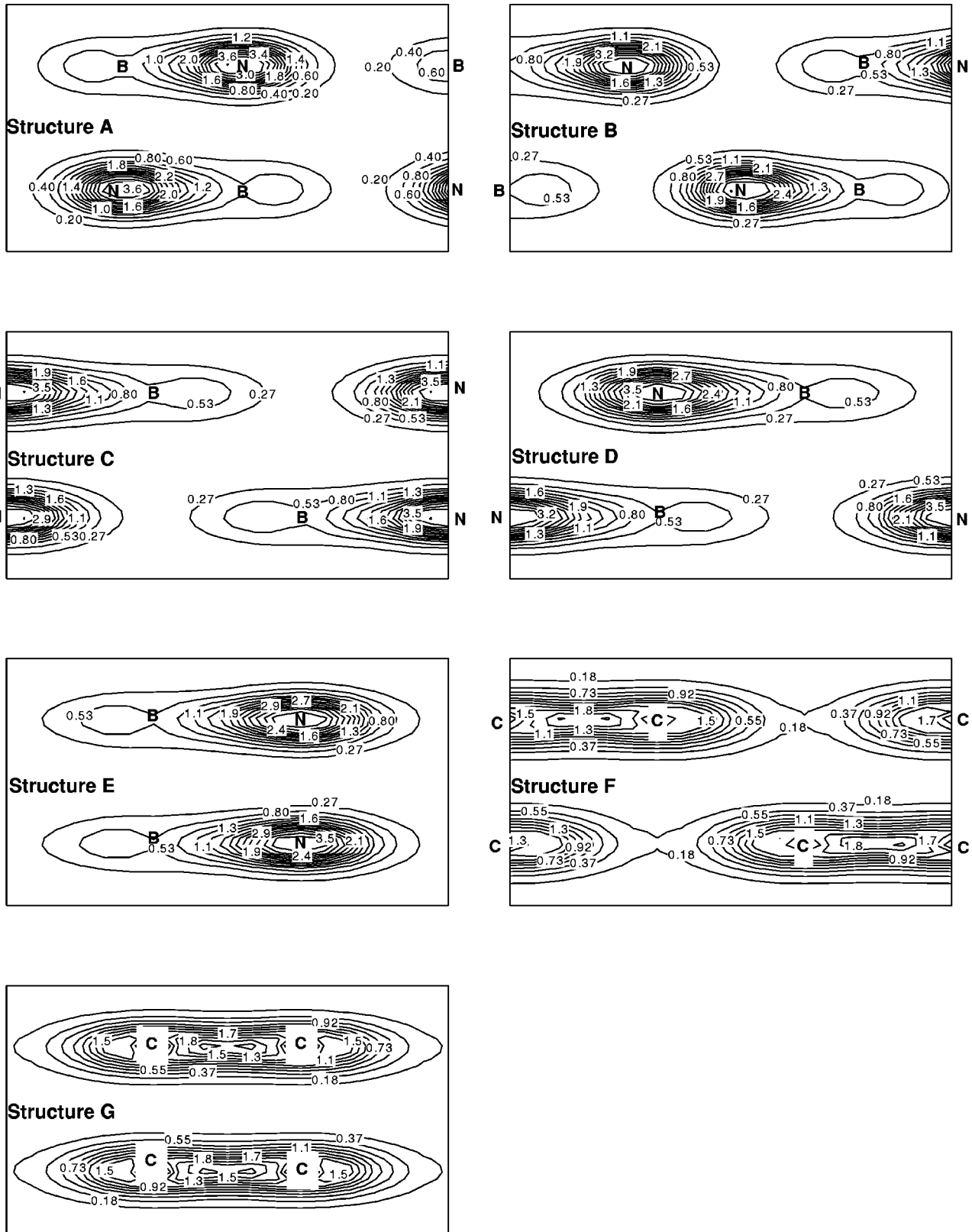
FIG. 3. Contour plots of total charge densities in the (1100) plane for the five *h*-BN and two graphitic structures being studied.

tures A, B, C, D, and E represent the extremes of stacking. Based on these, we can infer the structural or electronic properties of structures with disorder in stacking sequence such as PBN and *t*-BN. In PBN, stacking disorder typically occurs because PBN is often deposited with a preferred orientation and the *c* axis is perpendicular to the surface, resulting in slightly higher (2%–4%) interlayer spacing.[16] Similarly, in *t*-BN which has random stacking of the BN basal
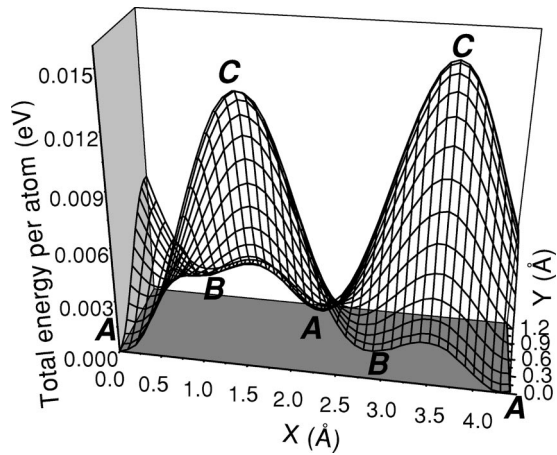
FIG. 4. Variation of total energy per atom of group-I structures as a function of the translational gliding move of one BN hexagonal layer relative to the other in the unit cell.

layers, a larger than the ideal d_{002} value in XRD analysis is often used as an indicator for the turbostratic structure, and dropping of this quantity to a certain critical value during heat treatments was accepted as an indicator for ordering in the crystal structure.[20] Based on the results of the present study, we conclude that the larger interlayer spacing of PBN and t-BN is due to their mixed stacking behaviors since our calculations suggest that "bad" stacking results in larger lattice constant c.

The existence of a substable structure B is significant. The small difference in total energies of structure A and structure B implies that it is possible for h-BN crystals with the $P6_3/mmc$ symmetry to have mixed stacking behaviors of structures A and B, resulting in an intrinsic stacking fault in real h-BN crystals. Furthermore, once h-BN with the $P6_3/mmc$ symmetry is formed, it is difficult to transform into structure D with the $P3m1$ symmetry, and vice versa, because a much larger energy barrier must be overcome by the rotational motion in order to transform the crystal struc-
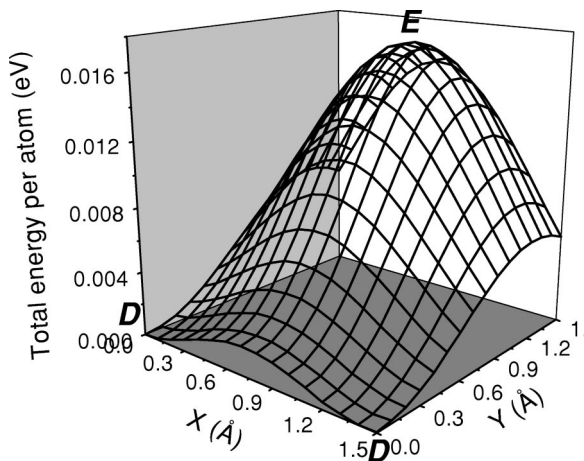

FIG. 5. Variation of total energy per atom of group-II structures as a function of the translational gliding move of one BN hexagonal layer relative to the other in the unit cell.
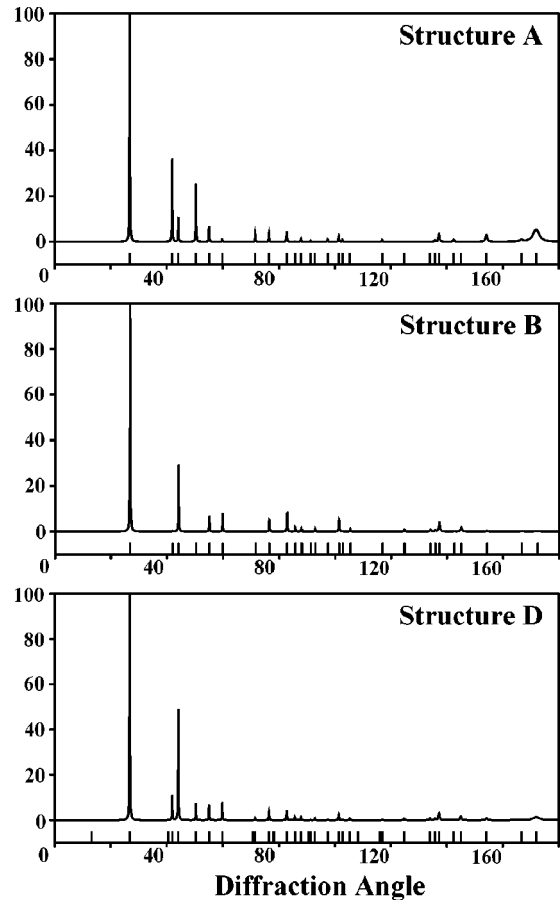

FIG. 6. Simulated XRD spectra of the stable structures A, B, and D, respectively ($\lambda = 1.5418$ Å).

ture from one symmetry to the other. Therefore, we conclude that whether h-BN crystals adopt the $P6_3/mmc$ or the $P3m1$ symmetry should be determined by their initial growth conditions.

Shown in Fig. 6 are the simulated XRD spectra based on the h-BN structures A, B, and D, respectively. Since these three structures have roughly the same lattice parameters, their XRD spectra have almost the same peak positions, but different intensities which is due to the different stacking of the BN layers. The experimental XRD spectra on real h-BN samples[52–58] are some sort of average of the spectra of the three ideal h-BN structures which confirms the existence of mixed stacking in real h-BN crystals.

III. ELECTRICAL PROPERTIES OF h-BN

The band structures and total density of states (DOS) of the five h-BN structures were calculated and are shown in Figs. 7–11. It is known that even though the DFT-LDA method underestimates band gaps of semiconductors and insulators, it does give reliable bandwidths and shapes. In the present work, we focus on comparison of the band structures of the five h-BNs.

Figure 7 shows the calculated band structure and total DOS of structure A. The band structure is characterized by
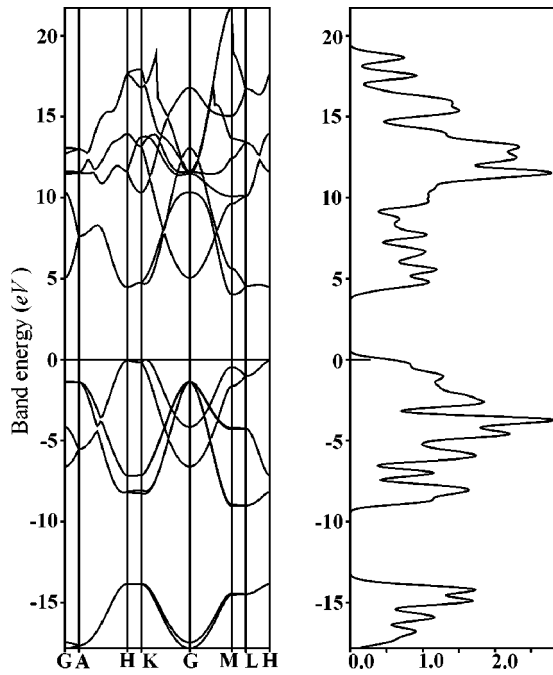
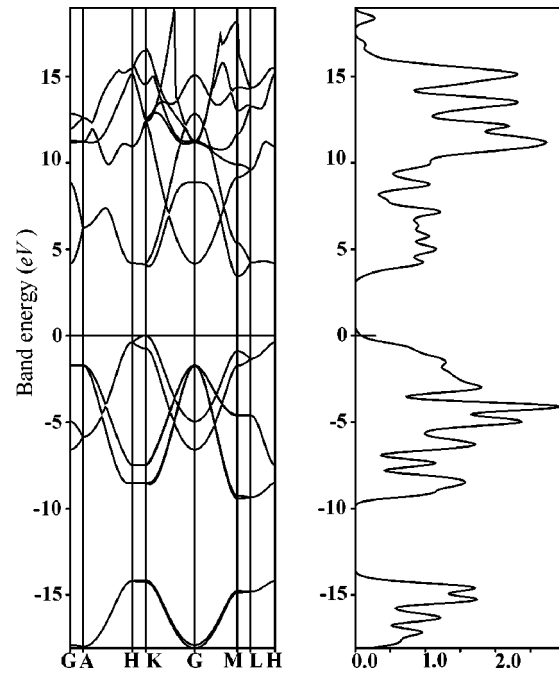FIG. 7. Band structure and total DOS of structure A.

FIG. 9. Band structure and total DOS of structure D.

an indirect band gap of about 4.027 eV, between the valence-band maximum near H and the conduction-band minimum at M, and a very small K-H dispersion. Being the most common h-BN phase, the electronic structure of structure A has been extensively studied.[42–46] The band structure calculated in the present work and the prediction of an indirect band gap of 4.027 eV agree well with the results of recent OL-CAO calculations of Xu and Ching[45] and the results of

Furthmüller *et al.* using ultrasoft pseudopotentials.[46]

For the substable structure B with the $P6_3/mmc$ symmetry, our calculations predict a band gap of about 3.395 eV, essentially of direct nature, which has not been observed before. The details of the valence-band top are shown in the inset of Fig. 8. The conduction-band minimum occurs at the K point, while the valence-band maximum is also located around the K point. The K-Γ dispersion is considerably small and is comparable to the thermal energy at room tempera-
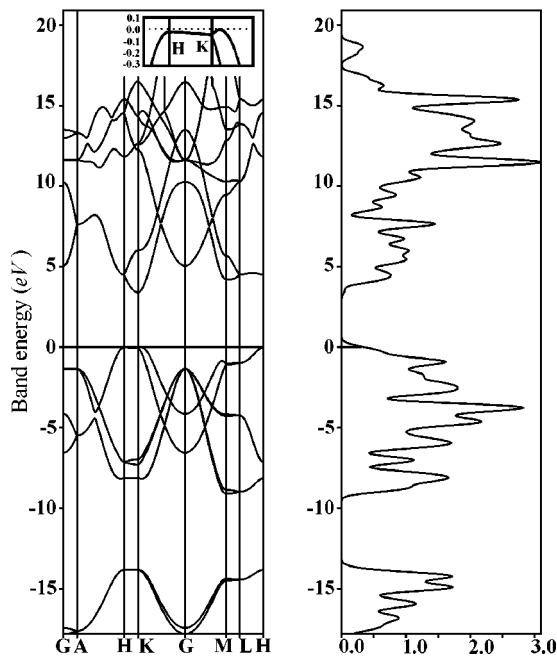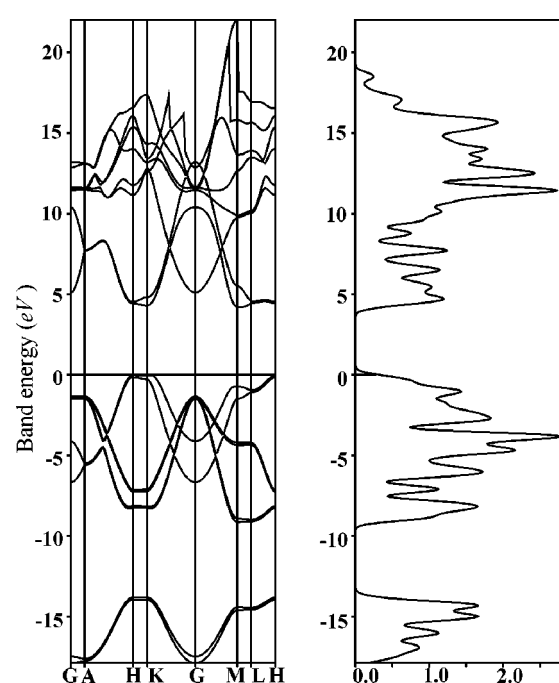

FIG. 8. Band structure and total DOS of structure B, where the K-H dispersion part is enlarged.

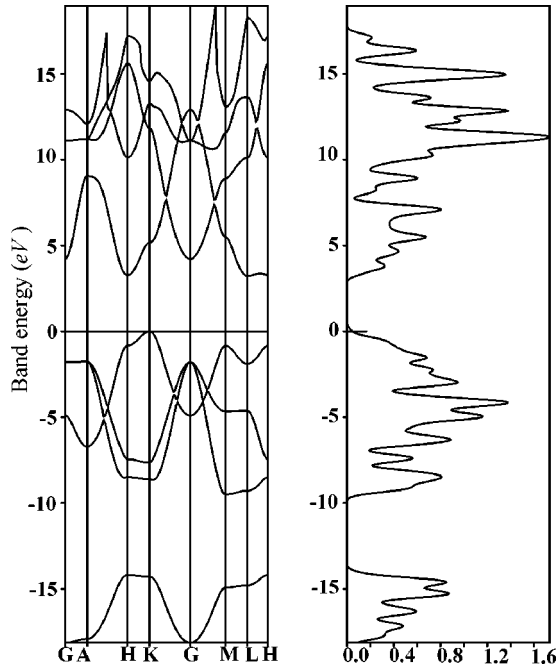FIG. 10. Band structure and total DOS of structure C.

FIG. 11. Band structure and total DOS of structure E.

ture. Therefore, the existence of structure B changes the nature of the electronic structure of h-BN and brings about a critical change from the indirect band gap to direct band gap, with a drop of the band-gap energy by about 0.6 eV.

The band structure of structure D with the $P3m1$ symmetry was calculated and is shown in Fig. 9. The band structure is similar to that of structure A, with an indirect but a slightly large band gap of 4.208 eV, between the valence-band maximum at H and the conduction band minimum at M, with very small K-H dispersion too.

For comparison, we also calculated the band structures of the unstable h-BN structures C and E and the results are shown in Fig. 10 and Fig. 11, respectively. Both of these two unstable structures with "bad" stacking sequences exhibit indirect band gaps. The band-gap energy of structure C is 3.433 eV, between the valence-band maximum at K and the conduction-band minimum at M, while that of structure E is 3.226 eV, between the valence-band maximum at K and the conduction-band minimum at L. Consequently, any "bad" stacking of BN layers in real h-BN would reduce its band gap, and change the characteristics of the band structure significantly.

Based on the calculated band structures of various phases of h-BN, it is obvious that the electronic structures of h-BN show strong dependence on the stacking manner of the BN layers. Structures with "good" stacking sequences already have quite dispersed band-gap energies, i.e., 4.027, 3.395, and 4.208 eV for structures A, B, and D, respectively. The existence of "bad" stacking of the BN layers such as that in structure C or E will further reduce their band-gap energy, and change their band structure. It is worthwhile to point out that the substable structure B possesses a totally different electronic structure and it is the only h-BN structure with a direct band gap. As already indicated in Sec. II, intrinsic

stacking faults should generally exist in real h-BN crystals. In other words, real h-BN crystals are likely to have mixed stacking sequences of structures A, B, and D. Accordingly, the diverse band-gap values (3.6 to 7.1 eV) observed experimentally[22] can be understood as a result of band-structure variation due to stacking. Furthermore, the discrepancy over the nature of the band gap, whether it is direct band gap[38] or indirect band gap,[22] can be attributed to the existence of the substable structure B. The relative dominance of stacking sequence A or stacking sequence B in a given h-BN will determine whether it is an indirect or a direct band-gap material. The electronic property of h-BN can thus be fully understood.

Based on the calculated electronic structures, we can also speculate that a band gap much lower than that of normal h-BN should be observed for structures with disordered stacking sequences such as PBN and t-BN, due to the existence of the "bad" stacking behaviors. Furthermore, stacking effects on the band structure of h-BN would provide further insight into understanding the electronic and optical properties of h-BN, such as energy levels induced by defects or impurities, characteristics of luminescence, etc. The fact that the stacking sequence can be altered by gliding moves of BN layers suggests that tunable band structure can be achieved simply by applying shearing stress on the BN crystals.

IV. CONCLUSION

h-BN modifications due to stacking have been investigated thoroughly using the DFT-LDA method. First, five possible h-BN structures, i.e., structures A, B, and C with symmetry $P6_3/mmc$ in one group (I) and structures D with $P3m1$ and E with $P\bar6m2$ in another (group II) were studied. Structures A and D were found stable and structure B substable, all with "good" stacking of BN layers. Structures C and E were found unstable. These structures with "bad" stacking of BN layers have a longer lattice constant c compared to structures with "good" stacking sequences. Real h-BN crystals may have mixed stacking, and intrinsic stacking faults can be expected, which are the reasons for the large variations of electronic properties of h-BN. Stacking sequence disorder is also the origin for the observed larger interlayer spacings in PBN and t-BN.

Second, the electronic properties of h-BN were found to be strongly dependent on the stacking of the hexagonal BN layers. Based on the calculated band structures for various phases, we presented an complete explanation on the inconsistency in experimental electronic and optical properties of h-BN. The diverse band-gap values of h-BN observed experimentally now can be understood based on the variation of band structure due to stacking. The discrepancy in the band-gap characteristics of h-BN, i.e., being direct or indirect, can be attributed to the existence of the substable structure B. Finally, structures with disordered stacking such as PBN and t-BN were predicted to have a much lower band gap than that of a normal h-BN.

[1] S. Larach and R.E. Shrader, Phys. Rev. **102**, 582 (1956).

[2] S. Larach and R.E. Shrader, Phys. Rev. **104**, 68 (1956).

[3] L. Kleinman and J.C. Phillips, Phys. Rev. **117**, 460 (1960).

[4] R. Geick, C.H. Perry, and G. Rupprecht, Phys. Rev. **146**, 543 (1966).

[5] P.J. Gielisse, S.S. Mitra, J.N. Plendl, R.D. Griffis, L.C. Mansur, R. Marshall, and E.A. Pascoe, Phys. Rev. **155**, 1039 (1967).

[6] D.N. Bose and H.K. Henisch, J. Am. Ceram. Soc. **53**, 281 (1970).

[7] Q. Johnson and A.C. Mitchell, Phys. Rev. Lett. **29**, 1369 (1972).

[8] A.M. Dobrotvorskii and R.A. Evarestov, Phys. Status Solidi B **66**, 83 (1974).

[9] A. Katzir, J.T. Suss, A. Zunger, and A. Halperin, Phys. Rev. B **11**, 2370 (1975).

[10] A. Zunger and A. Katzir, Phys. Rev. B **11**, 2378 (1975).

[11] E.Y. Andrei, A. Katzir, and J.T. Suss, Phys. Rev. B **13**, 2831 (1976).

[12] F.C. Brown, R.Z. Bachrach, and M. Skibowski, Phys. Rev. B **13**, 2633 (1976).

[13] A. Zunger, A. Katzir, and A. Halperin, Phys. Rev. B **13**, 5560 (1976).

[14] W.H. Gust and D.A. Young, Phys. Rev. B **15**, 5012 (1977).

[15] Y.F. Tsay, A. Vaidyanathan, and S.S. Mitra, Phys. Rev. B **19**, 5422 (1979).

[16] J.H. Edgar, V.L. Solozhenko, V.V. Lopatin, W.R.L. Lambrecht, B. Segall, and G.L. Doll, in *Properties of Group III Nitrides*, edited by J.H. Edgar (INSPEC, London, 1994), pp. 7 and 43.

[17] C.K. Narula, *Ceramic Precursor Technology and Its Applications* (Marcel Dekker, New York, 1995).

[18] J.Y. Huang, H. Yasuda, and H. Mori, J. Am. Ceram. Soc. **83**, 403 (2000).

[19] J. Thomas, Jr., N.E. Wetston, and T.E. O'Connor, J. Am. Chem. Soc. **84**, 4619 (1963).

[20] S. Alkoy, C. Toy, T. Gönül, and A. Tekin, J. Eur. Ceram. Soc. **17**, 1415 (1997).

[21] T. Kobayashi, S. Tashiro, T. Sekine, and T. Sato, Chem. Mater. **9**, 233 (1997).

[22] V.L. Solozhenko, A.G. Lazarenko, J.-P. Petitet, and A.V. Kanaev, J. Phys. Chem. Solids **62**, 1331 (2001).

[23] P. Widmayer, H.-G. Boyen, P. Ziemann, P. Reinke, and P. Oelhafen, Phys. Rev. B **59**, 5233 (1999).

[24] C.A. Taylor II, S.W. Brown, V. Subramaniam, S. Kidner, S.C. Rand, and R. Clarke, Appl. Phys. Lett. **65**, 1251 (1994).

[25] R.D. Leapman and J. Silcox, Phys. Rev. Lett. **42**, 1361 (1979).

[26] R.D. Leapman, P.L. Fejes, and J. Silcox, Phys. Rev. B **28**, 2361 (1983).

[27] C. Tarrio and S.E. Schnatterly, Phys. Rev. B **40**, 7852 (1989).

[28] J. Barth, C. Kunz, and T.M. Zimkina, Solid State Commun. **36**, 453 (1980).

[29] E. Tegeler, N. Kosuch, G. Wiech, and A. Faessler, Phys. Status Solidi B **91**, 223 (1979).

[30] R.D. Carson and S.E. Schnatterly, Phys. Rev. Lett. **59**, 319 (1987).

[31] A. Mansour and S.E. Schnatterly, Phys. Rev. B **36**, 9234 (1987).

[32] B.M. Davies, F. Bassani, F.C. Brown, and C.G. Olson, Phys. Rev. B **24**, 3537 (1981).

[33] J.J. Jia, T.A. Callcott, E.L. Shirley, J.A. Carlisle, L.J. Terminello, A. Asfaw, D.L. Ederer, F.J. Himpser, and R.C.C. Perera, Phys. Rev. Lett. **76**, 4054 (1996).

[34] J.A. Carlisle, E.L. Shirley, L.J. Terminello, J.J. Jia, T.A. Callcott, D.L. Ederer, R.C.C. Perera, and F.J. Himpsel, Phys. Rev. B **59**, 7433 (1999).

[35] M.J. Rand and J.F. Roberts, J. Electrochem. Soc. **115**, 423 (1968).

[36] W. Baronian, Mater. Res. Bull. **7**, 119 (1972).

[37] J. Zupan and D. Kolar, J. Phys. Chem. **5**, 3097 (1972).

[38] D.M. Hoffman, G.L. Doll, and P.C. Eklund, Phys. Rev. B **30**, 6051 (1984).

[39] R. Mamy, J. Thomas, G. Jezequel, and J.C. Lemonnier, J. Phys. (France) Lett. **42**, 473 (1981).

[40] V.V. Lopatin and F.V. Konusov, J. Phys. Chem. Solids **53**, 847 (1992).

[41] L.G. Carpenter and P.Y. Kirby, J. Phys. D **15**, 1143 (1982).

[42] J. Robertson, Phys. Rev. B **29**, 2131 (1984).

[43] A. Catellani, M. Posternak, A. Baldereschi, and A.J. Freeman, Phys. Rev. B **36**, 6105 (1987).

[44] K.T. Park, K. Terakura, and N. Hamada, J. Phys. C **20**, 1241 (1987).

[45] Y.N. Xu and W.Y. Ching, Phys. Rev. B **44**, 7787 (1991).

[46] J. Furthmüller, J. Hafner, and G. Kresse, Phys. Rev. B **50**, 15 606 (1994).

[47] W. Orellana and H. Chacham, Phys. Rev. B **63**, 125205 (2001).

[48] I. Jiménez, A.F. Jankowski, L.J. Terminello, D.G.J. Sutherland, J.A. Carlisle, G.L. Doll, W.M. Tong, D.K. Shuh, and F.J. Himpsel, Phys. Rev. B **55**, 12 025 (1997).

[49] I. Tanaka, H. Araki, M. Yoshiya, T. Mizoguchi, K. Ogasawara, and H. Adachi, Phys. Rev. B **60**, 4944 (1999).

[50] R.S. Pease, Nature (London) **165**, 722 (1950).

[51] R.S. Pease, Acta Crystallogr. **5**, 356 (1952).

[52] JCPDS file number 34-0421, JCPDS International Center for Diffraction Data.

[53] JCPDS file number 45-0895, JCPDS International Center for Diffraction Data.

[54] JCPDS file number 73-2095, JCPDS International Center for Diffraction Data.

[55] JCPDS file number 45-0893, JCPDS International Center for Diffraction Data.

[56] JCPDS file number 45-0896, JCPDS International Center for Diffraction Data.

[57] JCPDS file number 74-1977, JCPDS International Center for Diffraction Data; JCPDS file number 74-1978, JCPDS International Center for Diffraction Data.

[58] JCPDS file number 85-1068, JCPDS International Center for Diffraction Data.

[59] T.E. Mosuang and J.E. Lowther, J. Phys. Chem. Solids **63**, 363 (2002).

[60] P. Hohenberg and W. Kohn, Phys. Rev. **136**, 864 (1964).

[61] W. Kohn and L.J. Sham, Phys. Rev. **140**, A1133 (1965).

[62] J.P. Perdew and A. Zunger, Phys. Rev. B **23**, 5048 (1981).

[63] M.C. Payne, M.P. Teter, D.C. Allan, T.A. Arias, and J.D. Joannopoulos, Rev. Mod. Phys. **64**, 1045 (1992).

[64] D. Vanderbilt, Phys. Rev. B **41**, 7892 (1990); K. Laasonen, R. Car, C. Lee, and D. Vanderbilt, *ibid.* **43**, 6796 (1991).